ELASTIC-PLASTIC MODEL OF ADHESIVE-BONDED COMPOSITE JOINTS

Hai Huang and Charles Yang

Department of Mechanical Engineering
Wichita State University
Wichita, Kansas 67260, USA

SUMMARY: An analytical model was developed to determine the stress and strain distributions of adhesive-bonded composite single-lap joints under tension. Laminated anisotropic plate theory was applied in the derivation of the governing equations of the two bonded laminates. The adhesive was assumed elastic-perfectly plastic and follows von Mises yield criterion. The entire coupled system was determined through the kinematics and force equilibrium of the adhesive and the adherends. The overall system of governing equations was solved by directly solving the differential equations with appropriate boundary conditions. Computer software Maple was used as the calculation tool in solving these equations. Results from the analytical model were verified with finite element analysis using ABAQUS and also compared with experimental results using specimens defined in ASTM D 3165 "Strength Properties of Adhesives in Shear by Tension Loading of Single-Lap-Joint Laminated Assemblies." Although all three failure modes of bonded joints, substrate failure, cohesive, and adhesive failure, were present as the test results, only cohesive failure mode was analyzed.

KEYWORDS: single lap joints, composite joints, adhesive joints,

INTRODUCTION

Advanced composite materials have been widely used due to their light weight and high corrosion resistance. In many of these applications, bolted joints have been replaced by adhesive-bonded joints because of the weight penalty and corrosion problems. Many certification-related issues become more important as the application of adhesive-bonded joints gains it popularity in the general aviation industry. The purpose of this investigation is to develop an analytical model to determine the stress distribution within an adhesive-bonded single-lap composite joint and to use the model to analyze and predict the joint strength.

The earlier studies on adhesive-bonded joints can be found from the review papers by Kutscha [1], Kutscha and Hofer [2], Matthews *et al.* [3], and Vinson [4]. When studying adhesive-bonded lap joints, the effects due to the rotation of the adherends were first taken into account by Goland and Reissner [5]. They introduced an equation to relate the bending moment of the adherend at the end of the overlap to the in-plane loading. The basic approach of the Goland and Reissner theory was based on beam theory, or rather, on cylindrically bent-plate theory which treated the overlap section as a beam of twice the thickness of the adherend. Hart-Smith [6-9] published a series of papers regarding single-lap, double-lap, scarf, and stepped-lap joints involving a continuum mechanics model in which the adherends were isotropic or anisotropic elastic, and the adhesive was modeled as elastic, elastic-plastic, or bielastic. Basically, classical plate theory was adopted during Hart-Smith's derivation. However, the effects of transverse shear deformation, which has been shown to be important when the span-to-depth ratio is small or when the transverse shear modulus is small (Reissner [10], and Reddy [11]), were not included in either Goland and Reissner or Hart-Smith's theories. Moreover, edge effects were neglected, and adhesive stresses were assumed constant through the thickness in most of the

analyses found in the literature.

Renton and Vinson [12] utilized a higher order formulation which includes the adherend transverse shear and normal strains to analyze adhesive-bonded joints. Their results were compared with photoelastic experiments and show excellent agreement except for local stress concentrations at the edges of the overlap region. Griffin *et al.* [13] researched adhesive-bonded composite pipe joints and developed a mathematical model on the stress-strain behavior of such joints. Yang *et al*. [14] studied double-lap composite joints under cantilevered bending and proposed a strain gap model to describe the stress-strain behavior. Yang and Pang [15,16] also proposed analytical models for adhesive-bonded composite single-lap joints under cylindrical bending and tension based on the laminated anisotropic plate theory. Their approach correlated the asymmetry of the adherend laminates as well as the effects due to the transverse shear deformation. More recently, Oplinger [17] studied single-lap joints with isotropic adherends and found that many of the predictions of the Goland-Reissner analysis are recovered in the limit of large adherend-to-adhesive layer thickness ratios, although substantial differences from the Goland-Reissner analysis can occur for relatively thin adherends.

Strength of adhesive-bonded double-lap composite joints were studied by Tong [18] in 1997. Due to the fact that the failure often occurs at the resin-fiber interface adjacent to the adhesive, Tong used a simplified one-dimensional model as well as finite element model in conjunction with several existing and new interlaminar failure criteria to predict the strength of the joints. In 1996, Adams and Davies [19] published the results based on their non-linear finite element analysis on single-lap adhesive-bonded joints of composite/steel and composite/ aluminum with different taper arrangement at the edges of the joints. Experimental study of the effects of adherend lay-up sequence on the joint strength following ASTM D 1002 was published by Thomas *et al*. [20] in 1998.

Failure of adhesive-bonded joints has been investigated by many researchers. Just to name a few, Linear Elastic Fracture Mechanics approach was used by Chai [21, 22], Chai and Chiang [23]. They used the Butterfly and the End-Notch Flexure adhesive bond specimens to establish a crack propagation criterion for adhesive bonds. Dynamic crack growth of bond was investigated by Needleman and Rosakis [24]. Finite element method has been widely used to analyze adhesive-bonded composite structures as well as adhesive-bonded repairs. Among these researchers, Charalambides, *et al*. [25, 26] studied the bonded-repairs under static and fatigue loading experimentally as well as using elastic plastic finite element models.

Although finite element analysis can solve many mechanical problems with different materials and configurations, analytical solutions are still required to perform parametric analyses such as optimization. In the present study, an analytical model was developed to determine the stress and strain distributions of adhesive-bonded composite single-lap joints under tension. The Laminated Anisotropic Plate Theory was applied in the derivation of the governing equations of the two bonded laminates. The adhesive was assumed to be very thin and the adhesive stresses were assumed constant through the bondline thickness. The composite adherends were assumed linear elastic while the adhesive was assumed elastic-perfectly plastic following von Mises yield criterion in the derivations. The entire coupled system was then determined through the kinematics and force equilibrium of the adhesive and the adherends. The overall system of governing equations was solved by analytically solving the differential equations with appropriate boundary conditions. Computer software Maple was used as the solution tool. Results from the analytical model were verified with finite element analysis using ABAQUS.

The three major failure modes of adhesive-bonded joints are (1) cohesive failure, (2) adhesive failure, and (3) adherend failure. While the third failure mode, which is the most common failure mode of bonded joints with angle-ply composite laminates, has been analyzed by the

authors [27], the focus of this current study is the cohesive failure mode. ASTM D 3165 specimen specification was used for both analytical model and experimental evaluations. Joint specimens with Hysol EA 9394 structural paste adhesive and both carbon/epoxy and glass/epoxy adherends were tested for strength. All failed joints were examined for failure mode and only the joints failed under cohesive failure mode were used for this present analysis. Joint failure criterion was proposed based on the experimental and analytical results.

MODEL DERIVATION

Figure 1 shows the configuration of a single-lap joint following ASTM D 3165 configuration which was used in the current investigation. The tensile load, defined as *P*, represents the load per unit width. The joint was divided into three regions for convenience in the model development.

Adherend Formulation

The generalized formulas of the adherend and adhesive are the same for all three regions. The upper and lower adherends are assumed to follow the first-order laminated plate theory. The displacement field of the two adherends, *u* in the *x*-direction and *w* in the *z*-direction, can be written as

$$u^{U} = u^{oU}(x) + z^{U}\,\psi^{U}(x) \quad \textbf{(1)}$$

$$u^{L} = u^{oL}(x) + z^{L}\,\psi^{L}(x) \quad \textbf{(2)}$$

$$w^{U} = w^{U}(x) \quad \textbf{(3)}$$

$$w^{L} = w^{L}(x) \quad \textbf{(4)}$$

where superscript *U* and *L* denote the upper and lower adherend, respectively, superscript *o* represents the mid-plane displacement, and ψ is the corresponding bending slope. After substituting Eqs. (1) - (4) into the strain-displacement relations together with the equivalent modulus matrices [*A*], [*B*], and [*D*] for orthotropic laminates, the normal stress resultant N_x, bending moment for unit width M_y, and transverse shear stress resultant Q_z, can be obtained as

$$N_x = A_{11}\frac{du^{o}(x)}{dx} + B_{11}\frac{d\psi(x)}{dx} \quad \textbf{(5)}$$

$$M_y = B_{11}\frac{du^{o}(x)}{dx} + D_{11}\frac{d\psi(x)}{dx} \quad \textbf{(6)}$$

$$Q_z = kA_{55}\left(\psi(x) + \frac{dw(x)}{dx}\right) \quad \textbf{(7)}$$

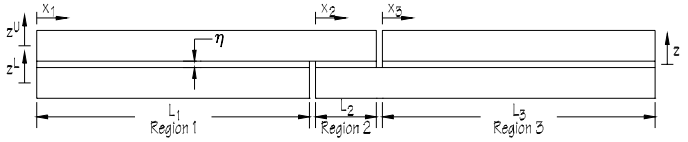

Figure 1 Joint Configuration and Coordinate Systems

In order to establish the equations of equilibrium, a free body diagram of the laminates and adhesive is shown in Fig. 2. The equations for force equilibrium are then

$$\frac{dN_x^{U}}{dx} = -\tau_{xz} \quad \textbf{(8)}$$

$$\frac{dM_y^{U}}{dx} = Q_z^{U} + \frac{h^{U}}{2}\tau_{xz} \quad \textbf{(9)}$$

$$\frac{dQ_z^{\,U}}{dx} = \sigma_z \tag{10}$$

where τ_{xz} and σ_z are the shear and peel stresses of the adhesive and h^U is the thickness of the upper adhrerend. Three equilibrium equations can be obtained for the lower adherend in the same fashion.

Adhesive Behavior in Elastic Regions

Assume a perfect bond between the adhesive and the adherend surfaces, based on the kinematics of the adhrends, the adhesive strains are related to the bottom surface of the upper laminate and the top surface of the lower adherend. In terms of the displacement field of the two laminates, the adhesive strains can be written as

$$\gamma_{xz} = \left[(u^{oL} - u^{oU}) + \left(\frac{h^L}{2}\psi^L + \frac{h^U}{2}\psi^U\right) - \left(\frac{dw^L}{dx} + \frac{dw^U}{dx}\right) \right] / \eta \tag{11}$$

$$\varepsilon_x = \frac{1}{2}\frac{d}{dx}\left[(u^{oL} + u^{oU}) + \left(\frac{h^L}{2}\psi^L - \frac{h^U}{2}\psi^U\right) \right] \tag{12}$$

$$\varepsilon_z = \frac{1}{2}(w^U - w^L) \tag{13}$$

where η is the adhesive thickness. Under plane strain condition, the adhesive stresses can be obtained as

$$\sigma_x = \frac{E}{(1+\nu)(1-2\nu)}\left[(1-\nu)\varepsilon_x + \nu\varepsilon_z\right] \tag{14}$$

$$\sigma_x = \frac{\nu E}{(1+\nu)(1-2\nu)}(\varepsilon_x + \varepsilon_z) \tag{15}$$

$$\sigma_z = \frac{E}{(1+\nu)(1-2\nu)}\left[\nu\varepsilon_x + (1-\nu)\varepsilon_z\right] \tag{16}$$

and

$$\tau_{xz} = G\gamma_{xz} \tag{17}$$

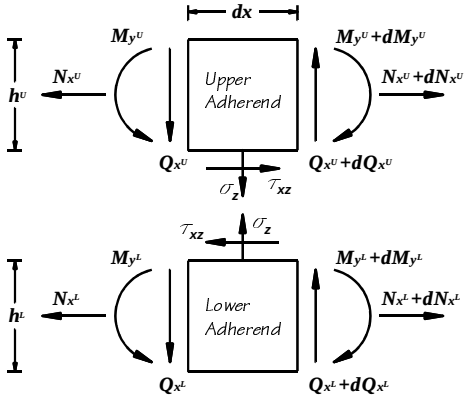

Figure 2 Free Body Diagram and Sign Conventions

Adhesive Behavior in Plastic Regions

High adhesive stresses at the vicinity of the joint edges are expected. Therefore, it is necessary to assume a plastic zone near each of the edges where adhesive yielding is considered.

Based on Prandtl-Reuss material model, the plastic strain increment is expressed by the flow rule

$$d\varepsilon_{ij}^{p} = \frac{\partial g}{\partial \sigma_{ij}}\, d\lambda \tag{18}$$

where ε_{ij} and σ_{ij} are the strain and stress tensor of the adhesive, respectively, and g is plastic potential. When elastic-perfectly plastic behavior following von Mises yield criterion is assumed for the adhesive, the plastic potential can be assumed as

$$g = J_2 = \frac{1}{2}\, s_{ij} s_{ji} \tag{19}$$

Therefore, Eq. (18) can be written as

$$\frac{d\varepsilon_x^p}{s_x} = \frac{d\varepsilon_y^p}{s_y} = \frac{d\varepsilon_z^p}{s_z} = \frac{d\gamma_{xy}^p}{\tau_{xy}} = \frac{d\gamma_{yz}^p}{\tau_{yz}} = \frac{d\gamma_{zx}^p}{\tau_{zx}} = d\lambda \tag{20}$$

Also, for an perfectly plastic material

$$d\sigma_{ij} = 2G de_{ij} + K d\varepsilon_{kk}\delta_{ij} - \frac{G s_{mn} de_{mn}}{k^2} s_{ij} \tag{21}$$

where e_{ij} is the deviatoric strain tensor, δ_{ij} is the *Kronecker delta*, $k = (J_2)^{1/2}$, G is the shear modulus, and

$$K = \frac{E}{3(1-2\nu)} \tag{22}$$

von Mises stress σ' can be expressed in terms of deviatoric stresses and shear stresses as

$$\sigma' = \sqrt{\frac{3}{2}(s_x^2 + s_y^2 + s_z^2) + \tau_{xz}^2} \tag{23}$$

By assuming the shear stress τ_{xz} is much greater than all the three deviatoric stress components when the adhesive reaches the yield stress at the edges of the joint,

$$\tau_{xz} = \frac{\sigma_{yield}}{\sqrt{3}} \tag{24}$$

and

$$s_x \approx 0 \qquad s_y \approx 0 \qquad s_z \approx 0 \tag{25}$$

Based on this assumption and Eq. (21), it can shown that $d\sigma_x \approx d\sigma_y \approx d\sigma_z \approx 0$. Therefore, the adhesive behavior in the plastic zones are

$$\sigma_x = \frac{E}{(1+\nu)(1-2\nu)}\left[(1-\nu)\varepsilon_x + \nu\varepsilon_z\right] \tag{26}$$

$$\sigma_y = \frac{\nu E}{(1+\nu)(1-2\nu)}(\varepsilon_x + \varepsilon_z) \tag{27}$$

$$\sigma_z = \frac{E}{(1+\nu)(1-2\nu)}\left[\nu\varepsilon_x + (1-\nu)\varepsilon_z\right] \tag{28}$$

and

$$\tau_{xz} = \tau_p = \frac{\sigma_{yield}}{\sqrt{3}} \tag{29}$$

This assumption has been verified by an finite element analysis using ABAQUS. Figure 3 shows the adhesive stress distribution in Region 2 as specified in Fig. 1. It can seen that the shear stress is almost constant with the yield zones while the von Mises stress remains constant.

Because the adhesive shear stress is assumed constant within the yield zone, the von Mises stress calculated based on in Eq. (23) is no longer a constant. A factor is then applied to each of the stress components to scale down the von Mises stress to the value of the yield stress σ_{yield}.

SOLUTION PROCEDURE

The overall system of governing equation includes eighteen (18) coupled second-order ordinary

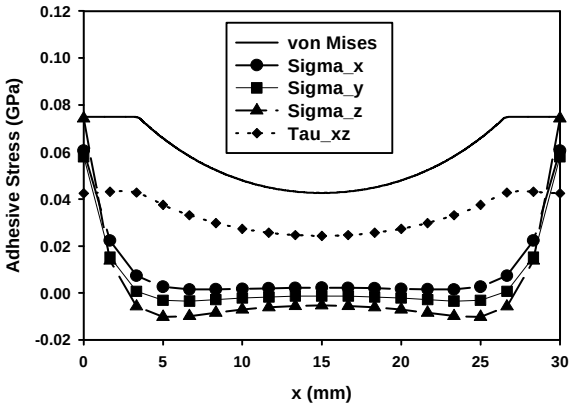

Figure 3 Adhesive Stress Distribution from FEM (ABAQUS)

equations with eighteen (18) variables. A total of thirty six (36) boundary conditions are obtained at the ends of each joint regions as shown in Fig. 1 from either continuity or applied force conditions. Solutions are obtained by using a symbolic solver, Maple V [28], with the Laplace option. Once the Laplace option is chosen, Maple V performs forward and inverse Laplace transformations to obtain the exact solutions to the system of ordinary differential equations.

RESULTS AND DISCUSSION

In order to demonstration the application of the developed model, a joint system as described in Fig. 1 was modeled used both the developed model and finite element software ABAQUS. In this illustration, T300/5208 (Graphite/Epoxy) with ply thickness 0.25 mm was used for both upper and lower adherends. Each adherend consists of 12 plies with orientation and sequence $[0_3/90_3]_S$. The engineering constants of T300/5208 are

$$E_{11} = 181 \text{ GPa} \quad E_{22} = 10.3 \text{ GPa} \quad G_{12} = 7.17 \text{ GPa} \quad \nu_{12} = 0.28$$

For convenience, other mechanical properties of the adherends are assumed as $E_{33} = E_{22}$, $G_{13} = G_{12}$, $\nu_{13} = \nu_{12}$, $\nu_{23} = 0.35$, and $G_{23} = E_{22}/2(1+\nu_{23}) = 3.815$ GPa. Based on the material properties above, the mechanical constants of the adherends per unit width can be given as

$$A_{11}{}^{U} = A_{11}{}^{L} = 374 \text{ kN/mm} \qquad B_{11}{}^{U} = B_{11}{}^{L} = 0$$
$$D_{11}{}^{U} = D_{11}{}^{L} = 394 \text{ kNmm} \qquad A_{55}{}^{U} = A_{55}{}^{L} = 18.\,2\text{kN/mm}$$

The adhesive was Metbond 408 with the following properties

$$E = 0.96 \text{ GPa} \qquad G = 0.34 \text{ GPa}$$
$$\nu = 0.41 \qquad \sigma_{yield} = 0.0075 \text{ Gpa}$$

The joint dimensions include $L_1 = L_3 = 80$ mm, $L_2 = 30$ mm, and $\eta = 0.2$ mm. The applied tensile load was $P = 0.1$ kN/mm.

Figure 4 shows the von Mises stress distribution obtained from both the developed model and finite element model. A good correlation can be seen from the size of the yield zone and the

stress level in the entire joint region. Figure 5 and 6 show the adhesive peel stress (σ_z) and shear stress distributions, respectively, from the developed model and finite element model. It can be seen that after the scaling described previously, the lower value of shear stress at the ends of the joint was simulated by the developed model.

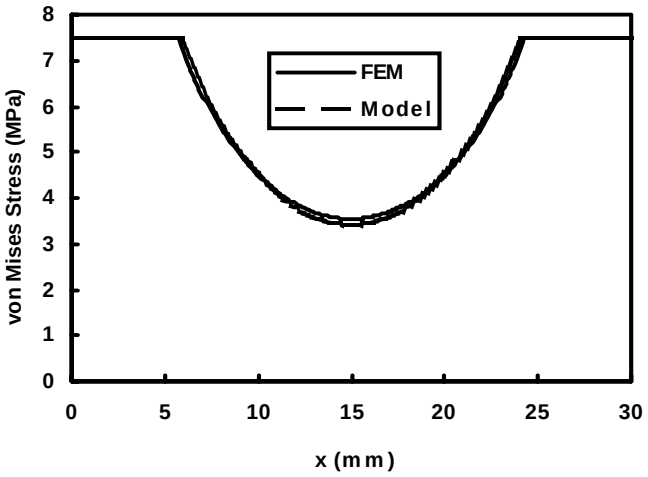

Figure 4 Adhesive von Mises Stress Distribution

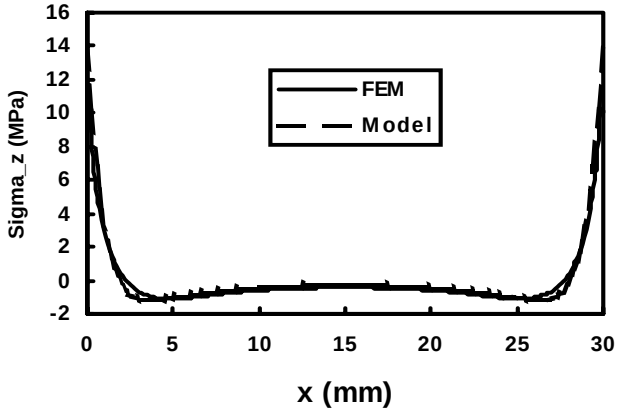

Figure 5 Adhesive Peel Stress Distribution

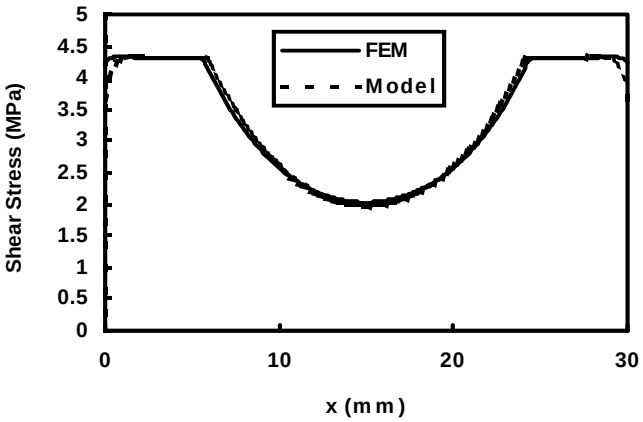

Figure 6 Adhesive Shear Stress Distribution

The joint strength can predicted once a suitable joint failure criterion is established. Several proposed criteria include (1) the hydrastatic stress at certain location – such as 5% of overlap length from the edges of the joint, (2) the average hydrastatic stress over certain percentage of the overlap length, and (3) the average plastic strain over certain percentage of the overlap length. The results all show good correlation with test results.

Several failure indexes are used to define the failure of the joint. The first index uses the hydrostatic stress of the adhesive at certain location of the overlap.

$$Index_1 = \frac{1}{3}(\sigma_x + \sigma_y + \sigma_z) \quad \textbf{(30)}$$

Table 1 provides the $Index_1$ value at α% of L_2 from the overlap edge using test results.

Table 1 $Index_1$ Values from Test Results

α	0	2	3	4	5
Sample #1	5.17	4.14	3.60	3.06	2.54
Sample #2	5.28	4.24	3.69	3.14	2.61
Sample #3	5.69	4.56	3.93	3.30	2.68
Sample #4	5.39	4.32	3.76	3.18	2.63
Sample #5	5.77	4.62	3.98	3..33	2.69
Average	5.46	4.38	3.79	3.21	2.62
Std. Dev.	0.261	0.204	0.162	0.111	0.058

If the average hydrostatic stress within certain length close to the edge of the overlap is used as failure criterion, $Index_2$ is written as

$$Index_2 = \frac{\int_0^{\alpha\beta} \frac{1}{3}(\sigma_x + \sigma_y + \sigma_z)dx}{\alpha\beta} \quad \textbf{(31)}$$

Table 2 $Index_2$ Values from Test Results

	β = Overlap Length		β = Adhesive Plastic Region		
α	5%	8%	10%	30%	50%
Sample #1	4.51	4.14	4.92	4.42	3.96
Sample #2	4.62	4.24	5.00	4.46	3.96
Sample #3	5.98	4.56	5.37	4.72	4.13
Sample #4	4.71	4.32	5.10	4.53	4.00
Sample #5	5.04	4.62	5.43	4.77	4.15
Average	4.77	4.38	5.16	4.58	4.01
Std. Dev.	0.229	0.207	0.226	0.157	0.081

If the average adhesive plastic strain is used to evaluate failure, $Index_3$ is

$$Index_3 = \frac{\int_0^{\alpha\beta} \gamma^p dx}{\alpha\beta} \quad \textbf{(32)}$$

Table 3 $Index_3$ Values from Test Results

	β = Overlap Length			β = Adhesive Plastic Region		
α	3%	5%	8%	10%	30%	50%
Sample #1	0.0435	0.0401	0.0353	0.0455	0.0389	0.0330
Sample #2	0.0480	0.0444	0.0395	0.0496	0.0423	0.0358
Sample #3	0.0640	0.0596	0.0533	0.0657	0.0557	0.0469
Sample #4	0.0517	0.0480	0.0427	0.0534	0.0454	0.0383
Sample #5	0.0675	0.0628	0.0562	0.0692	0.0585	0.0492
Average	0.0549	0.0510	0.0454	0.0567	0.0482	0.0406
Std. Dev.	0.0104	0.0098	0.0090	0.0103	0.0085	0.0071

CONCLUSIONS

An analytical model for adhesive-bonded single-lap joints under tension has been developed based on the first-order laminated plate theory for the adherend and elastic-perfectly plastic behavior for the adhesive. Based on the developed model, closed-form solutions for stress distributions of both the laminates and the adhesive can be obtained. The proposed closed-form solutions are found to correlate with the solutions that were obtained through finite element model. Several joint failure criteria were proposed and were evaluated with experiment data.

ACKNOWLEDGMENT

This material is based upon work supported by the Federal Aviation Administration under the Airworthiness Assurance Center of Excellence Contract Number IA031.

REFERENCES

1. Kutscha, D. 1964, "Mechanics of Adhesive-Bonded Lap-Type Joints: Survey and Review," Technical Report AFML-TDR-64-298.
2 Kutscha, D., and Hofer, K. E. Jr. 1969, "Feasibility of Joining Advanced Composite Flight Vehicles," Technical Report AFML-TR-68-391.
3. Matthews, F. L., Kilty, P. F. and Goodwin, E. W., 1982, "A Review of the Strength of Joints in Fibre-Reinforced Plastics: Part 2 Adhesively Bonded Joints," Composites, pp. 29-37. Mechanical Properties of Adhesives for Use in the Design of Bonded Joints," Report No FPL-011 (US Forest Products Laboratory).
4. Vinson, J. R., 1989, "Adhesive Bonding of Polymer Composites," Polymer Engineering and Science, Vol. 29, pp. 1325-1331.
5. Goland, M., and E. Reissner, 1944, "The Stresses in Cemented Joints," Journal of Applied Mechanics, Vol. 11, pp.A-17-A-27.
6. Hart-Smith, L. J., 1973a, "Adhesive-Bonded Single-Lap Joints," Douglas Aircraft Co., NASA Langley Report CR 112236.
7. Hart-Smith, L. J., 1973b, "Adhesive-Bonded Double-Lap Joints," Douglas Aircraft Co., NASA Langley Report CR 112235.
8. Hart-Smith, L. J., 1973c "Adhesive-Bonded Scarf and Stepped-Lap Joints," Douglas Aircraft Co., NASA Langley Report CR 112237.
9. Hart-Smith, L. J., 1974, "Analysis and Design of Advanced Composite Bonded Joints," Douglas Aircraft Co., NASA Langley Report CR-2218.
10. Reissner, E., 1945, "The Effect of Transverse Shear Deformation on the Bending of Elastic Plates," Journal of Applied Mechanics, Vol. 12, A-69-A-77.
11. Reddy, J. N., 1984, "A Refined Nonlinear Theory of Plates with Transverse Shear Deformation," International Journal of Solids Structures, Vol. 20, pp. 881-896.
12. Renton, W. J., and Vinson, J. R., 1977, "Analysis of Adhesively Bonded Joints Between

Panels of Composite Materials," Journal of Applied Mechanics, Vol. 44, pp. 101-106.
13. Griffin, S. A., Pang, S. S., and Yang, C. 1991, "Strength Model of Adhesive Bonded Composite Pipe Joints under Tension," Polymer Engineering and Science, Vol. 31, pp. 533-538.
14. Yang, C., Pang, S. S., and Griffin, S. A., 1992, "Failure Analysis of Adhesive-Bonded Double-Lap Joints Under Cantilevered Bending," Polymer Engineering and Science, Vol. 32, pp. 632-640.
15. Yang, C., and Pang, S. S., 1993, "Stress-Strain Analysis of Single-Lap Composite Joints under Cylindrical Bending," Composites Engineering, Vol. 3, pp. 1051-1063.
16 Yang, C. and Pang, S.S., 1996, "Stress-Strain Analysis of Single-Lap Composite Joints under Tension," ASME Trans. - J. of Engineering Materials and Technology, V. 118, pp. 247 - 255.
17. Oplinger, D. W., 1994, "Effects of Adherend Deflections in Single Lap Joints," International Journal of Solids and Structures, Vol. 31, pp. 2565-2587.
18. Tong, L., 1997, "An Assessment of Failure Criteria to Predict the Strength of Adhesively Bonded Composite Double Lap Joints," J. of Reinforced Plastics and Composites, V. 16, No. 8, pp. 698-713.
19. Adams, R.D. and Davies, R., 1996, "Strength of Joints Involving Composites," J. Adhesion, V. 59, pp. 171-182.
20. Thomas, R., Garcia, F.J., and Adams, R.D., 1998, "Adhesive Joining of Composite Laminates," Plastics, Rubber, and Composite Processing and Applications, V. 27, No. 4, pp. 200-205.
21. Chai, H.1992. "Micromechanics of Shear Deformations in Cracked Bonded Joints," Int. J. Fracture, 58: 223-239.
22. Chai, H. 1993. "Deformation and Failure of Adhesive Bonds under Shear Loading," J. of Materials Science, 28: 494-506.
23. Chai, H. and M. Y. M. Chiang. 1996. "A Crack Propagation Criterion Based on Local Shear Strain in Adhesive Bonds Subjected to Shear," J. Mech. Phys. Solids, 44: 1669-1689.
24. Needleman, A., and A. J. Rosakis. 1999. "Effect of Bond Strength and Loading Rate on the Condition Governing the Attainment of Intersonic Crack Growth along Interfaces," J. Mech. and Phy. Solids, 47(12): 2411-2449.
25. Charalambides, M. N., R. Hardouin, A. J. Kinloch, and F. L. Matthews. 1998. "Adhesively-Bonded Repairs to Fiber-Composite Materials I: Experimental," Composites Part A, 29A: 1371-1381.
26. Charalambides, M. N., R. Hardouin, A. J. Kinloch, and F. L. Matthews. 1998. "Adhesively-Bonded Repairs to Fiber-Composite Materials II: Finite Element Modelling," Composites Part A, 29A: 1383-1396.
27. H. Hai, C. Yang, J. Tomblin, and P. Harter, "Stress and Failure Analyses of Adhesive-Bonded Composite Joints using ASTM D3165 Specimens," Proc. American Society for Composites 15th Annual Technical Conference, College Station, Texas, September 24-27, 2000.28.Monagan M. B., K. O. Geddes, K. M. Heal, G. Labahn, and S. Vorkoetter. 1996. Maple V Programming Guide, Springer-Verlag, New York.